

Sputtering: Experiment

Andreas Wucher*

Department of Physics, University of Duisburg-Essen
Lotharstr. 1, D-47048 Duisburg, Germany

Abstract

A few aspects of experiments on particle-induced sputtering of solid surfaces are reviewed. In the *linear cascade* regime, experimental observables like sputter yields, energy and angular distributions of sputtered material are reasonably well understood, but open questions remain as to the physical nature of the surface binding energy, the emission of clusters and the electronic excitation of sputtered particles. In the *spike* regime, the emission mechanisms appear to be less clear. This is illustrated by recollecting some recent experimental data on particle emission under polyatomic projectile ion bombardment. The sputtering of molecular solids, again particularly under polyatomic projectile bombardment, is briefly discussed in terms of surface analytical applications.

Contents

1	Introduction: Experimental Tools	406
2	The Linear Cascade Regime	408
2.1	Yields	408
2.2	Energy Distributions	411
2.3	Angular Distributions	413
2.4	Low Energy Bombardment	415
2.5	Cluster Emission	416
2.6	Excitation and Ionization	418
3	The Spike Regime	421
3.1	Yields	421

* E-mail: andreas.wucher@uni-due.de

3.2	Energy Distributions	422
3.3	Cluster Emission	423
3.4	Ionization and Excitation	424
3.5	Molecular Solids	425
4	Conclusions	427
	References	428

1. Introduction: Experimental Tools

As a consequence of its widespread application area, the fundamentals of sputtering have been extensively investigated for more than four decades. Important milestones leading to our current understanding of the mechanisms were the early experiments on sputter yields conducted in the sixties and seventies which have been compiled and reviewed by Andersen and Bay (1981). These data were mostly obtained by weight loss measurements employing either electromechanical or quartz crystal microbalances. Due to this experimental technique, most of the available data were taken under so-called *dynamic* conditions, i.e. at large projectile ion fluences, where possible influences of bombardment induced surface modifications like topography evolution, etc., are not always well known.

Additional information on the sputtering process has been obtained from the distributions of the emitted species with respect to their emission energy, angle, excitation and charge state. Particularly the energy distribution of sputtered particles has been investigated extensively, since it provides the ultimate proof of the non-equilibrium character of the emission process. Experimental techniques applied to the determination of emission energy distributions include the time-of-flight analysis of sputtered neutral particles using either mechanical shutters or pulsed projectile beams in connection with time resolved detection of the sputtered particles using either electron impact, resonant or non-resonant laser post-ionization. Usually, post-ionization is followed by mass selection using either electrodynamic mass filters or time-of-flight (ToF) spectrometers. A second class of experiments utilizes the Doppler shift of resonant transitions in the emitted particle using, for instance, laser induced fluorescence for detection. The third tool employed to investigate kinetic energy distributions is electrostatic energy analysis of the emitted particles. With only one recent exception, practically all published energy distribution data of secondary ions have been determined this way, employing various variants of electrostatic energy filters. For neutrals, the method has been combined with post-ionization techniques, mostly by electron impact.

The angular emission distributions of sputtered particles have been investigated by collecting the emitted material on a substrate which is later subjected to surface and thin film analysis. The drawback of this method is that it can only be used in dynamic mode, involving relatively large amounts of sputtered material. Moreover, the mass distribution of sputtered particles is not accessible. For the static analysis of emitted neutrals, a technique has been developed which is based on laser post-ionization in combination with the spatially resolved detection of the generated photoions. In combination with a pulsed projectile ion beam, this allows the angular and energy resolved detection of emitted neutrals (EARN) (Kobrin et al., 1986).

The excitation states of sputtered particles were probed by different methods, depending on the lifetime of the investigated state. Short-lived states, on one hand, are detected by optical spectroscopy of the emitted light (see Yu, 1991, for a review). It has been attempted many times to correlate the distance dependence of the detected photon yield with the emission energy spectrum of the ejected excited particles, but this method is largely disturbed by cascading transitions from higher-lying states and must be regarded unreliable. Doppler broadening of the emitted spectral lines has also been utilized for that purpose (Betz, 1987), but the observed shifts are small and therefore measured line profiles must be fitted by a known functional form of the emission energy distribution. Long-lived metastable states, on the other hand, are probed by the same resonant techniques as ground state particles, just using different resonances specific for the investigated state. Again, detection is made either by laser induced fluorescence or by photoionization and subsequent ToF mass spectrometry.

The purpose of the present paper is not to attempt a comprehensive review of all data and information about sputtering phenomena that have been collected over many years using the above mentioned experimental techniques. In fact, there are a number of extensive reviews the reader is referred to in this respect (see, for instance, "Sputtering by Particle Bombardment", Vols. 1–3 and the upcoming Vol. 4, ed. R. Behrisch et al.). Instead, focus will be given to a few aspects where active research is currently being pursued. In the linear cascade regime, most of the fundamental mechanistic concepts are understood and reasonably good agreement has been achieved between experimental data and theory (Urbassek, 2006). This will be illustrated on a few examples, and a few open questions will be highlighted which still appear to be unsolved after many years of investigation. In the spike regime of collisional sputtering, even the fundamental concepts of bombardment induced particle emission have not been completely understood yet. This will be illustrated in terms of recent data collected for impact of polyatomic or "cluster" projectiles onto either simple elemental or molecular solids. Due to

the fact that (i) neutral particles make up the majority of the sputtered flux and (ii) secondary ion emission may be significantly influenced by ambiguities related to the ionization probability of a sputtered particle, the analysis will be restricted to experimental data obtained for sputtered *neutral* particles. Moreover, the scope of the present paper will be restricted to collisional sputtering phenomena, and electronic sputtering, which occurs at high impact energies or in special target materials like ionic crystals, is therefore not treated here.

2. The Linear Cascade Regime

As outlined in many reviews of sputtering, the concept of linear collision cascades involves a series of binary, mostly elastic collisions to distribute the energy imparted by the projectile among the solid constituents. Linearity is ensured by a low density of moving particles, and therefore each collision can be assumed to occur between a moving particle and a particle at rest. It is important to note that, if more than one of such cascades overlap in space and time, the result will simply be the sum of the effects produced by each cascade (or projectile impact) alone. Every deviation from this expectation will in the following be called a “nonlinear effect”. The theory of sputtering in this regime is well developed and found to agree reasonably well with corresponding experimental data (Urbassek, 2006). As a rule of thumb, linear collision cascades are produced if not too heavy projectiles of medium kinetic energies impinge onto surfaces of sufficiently strongly bound solids. A good example of this category is the impact of keV Ar^+ ions onto metallic or semiconductor surfaces.

2.1. YIELDS

There is an abundant volume of sputtering yield data which has been collected in the linear cascade regime of sputtering, a review of which can be found in the compilation of Andersen and Bay (1981). For elemental target material, the available experimental data have been analyzed in terms of functional forms derived from analytical transport theory, resulting in fit formulae and parameters (Matsunami et al., 1984) which can be used to estimate an unknown yield. For the case of metal targets, these appear to work reasonably well, allowing a prediction within an accuracy of typically a factor of two over a wide range of impact energies. As an example, Figure 1 shows measured data for polycrystalline copper along with the Matsunami fit formula (Matsunami et al., 1984) which can also be found on the web (<http://www.ss.teen.setsunan.ac.jp/e-syb.html>) (solid lines). A similarly good description of the data is provided by analytic sputtering theory

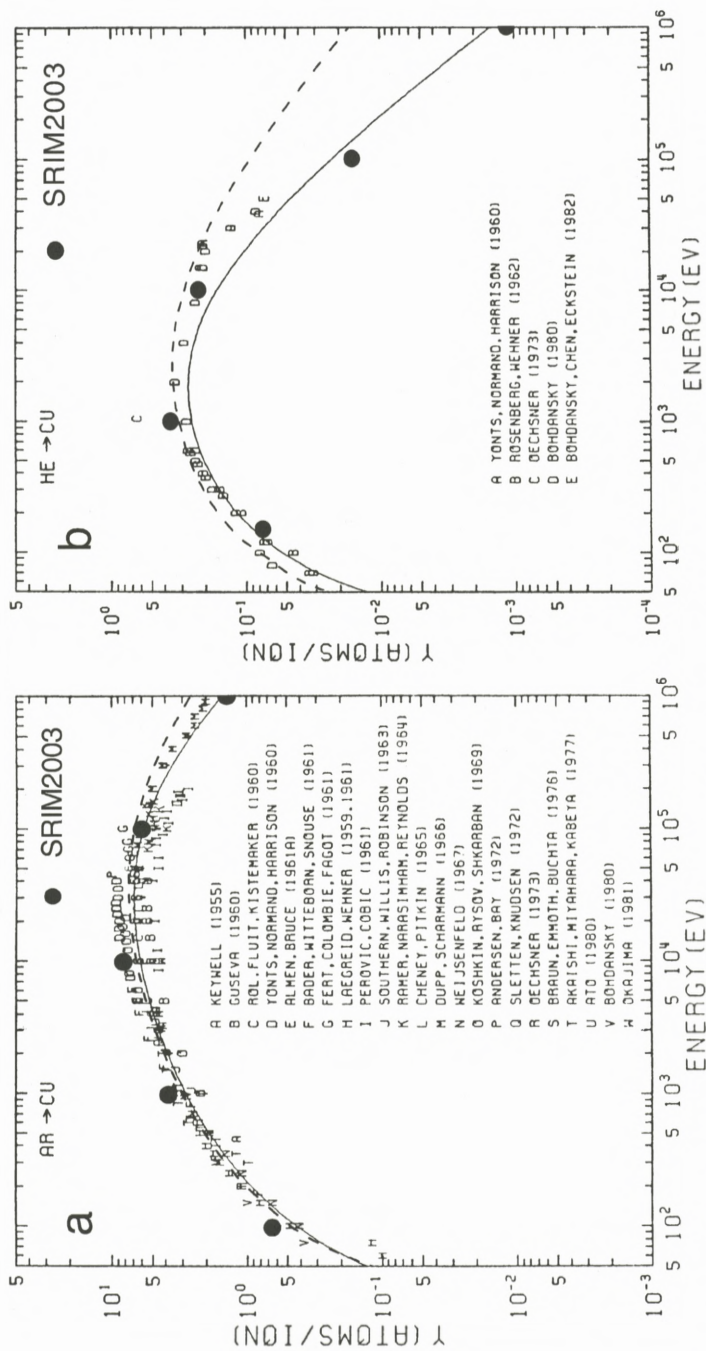


Figure 1. Experimental sputter yield data of polycrystalline Cu bombarded with various projectiles and kinetic energies under normal incidence (reproduced from Matsumami et al., 1984). Solid line: Matsumami fit formula; Dashed line: analytic sputtering theory; Large dots: Calculated values using the Monte Carlo computer simulation code SRIM 2003.

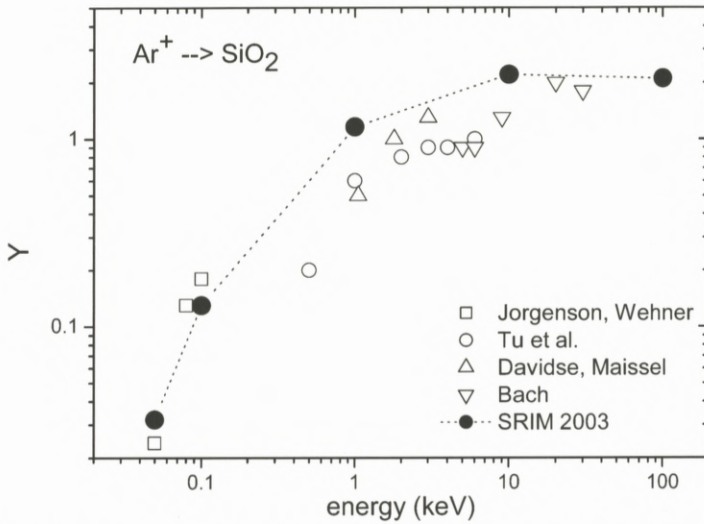


Figure 2. Sputter yield of SiO_2 under Ar^+ bombardment. Open symbols: experimental data taken from Jorgenson et al. (1965) (\square), Tu et al. (1980) (\circ), Davidse and Maisel, 1967 (\triangle) and Bach (1970) and Bach et al. (1974) (∇). Closed symbols: SRIM 2003 calculation.

(Sigmund, 1969) as implemented in Wittmaack (2003) (dashed lines). For comparison, the results of Monte-Carlo (MC) computer simulation using the SRIM 2003 program package (<http://www.srim.org>) are included as large dots.

The situation is not as clear if multicomponent materials are bombarded. Here, the surface composition is often changed due to preferential sputtering, bombardment induced mixing, surface segregation, etc., and the sputter yield will therefore exhibit a strong dependence on ion fluence (for a review, see Betz and Wehner, 1983; Sigmund and Lam, 1993). Moreover, the phase structure of the bombarded material will exert a large influence on the development of ion induced surface topography. As a consequence, the actual system will in general be much different from what is assumed in theoretical approaches (e.g. ideally flat surface, homogenous spatial distribution of constituents, unchanged surface composition, etc.). Experimentally, much less data exist on sputtering yields of this kind of materials, and no tool has been published which allows an accurate estimate of unknown yield values. One can of course use MC computer simulation (SRIM 2003) to make a prediction. For Ar^+ bombardment of SiO_2 , the result is depicted in Figure 2, which shows the so-called total sputter yield, i.e., the number of atoms (regardless of species) emitted per projectile impact. This particular example was chosen here because it represents a case for which a relatively

large set of experimental data exist. The yield calculated with SRIM 2003 appears to be systematically too high, a finding which is understandable since the MC simulation refers to the “static” case, i.e., the limit of negligible projectile fluence, whereas the yields are measured under “dynamic” conditions which result in a modified surface stoichiometry. In fact, the evaluation of total sputter yields from experiments measuring, for instance, the mass loss under ion bombardment is only meaningful under dynamic equilibrium conditions, where the surface composition has adjusted in such a way as to ensure stoichiometric sputtering of all sample constituents. Nevertheless, the data depicted in Figure 2 indicate again that the yield can be predicted within an accuracy of roughly a factor of two. It should be stressed, however, that SiO_2 may represent a very favorable case which certainly cannot be generalized. This is particularly true for multiphase alloys, and therefore great care should be taken in predicting sputter yields of multicomponent targets.

2.2. ENERGY DISTRIBUTIONS

The emission energy distribution of atoms sputtered from elemental targets has been measured many times. In general, the experimental data can be well approximated by the transport theory prediction (Thompson, 1968; Sigmund, 1981)

$$f(E) \propto \frac{E}{(E + U)^{3-2m}}, \quad (1)$$

using the surface binding energy U as a fitting parameter. The parameter m in the exponent is either assumed as zero or sometimes also treated as a parameter. Examples of measured energy distributions of neutral atoms sputtered from the respective elemental surfaces are shown in Figure 3. The data have been obtained using three different experimental methods on three different projectile-target combinations. It is seen that the surface binding energy parameter U is of the same order of magnitude as the sublimation energy of the solid. However, the agreement between both quantities is not perfect, a finding which is not surprising in view of the strong non-equilibrium nature of the emission process. In fact, it has been suggested that the acquisition of energy distributions as depicted in Figure 3 should represent an experimental approach to the determination of surface binding energies relevant in sputtering. So far, however, such an assessment does not appear to be unambiguously possible due to the large uncertainty of measured energy distributions particularly in the low energy range. This is illustrated in Figure 4, which shows the fit parameter U extracted from published energy distributions of sputtered neutral atoms as a function of the sublimation energy of the respective

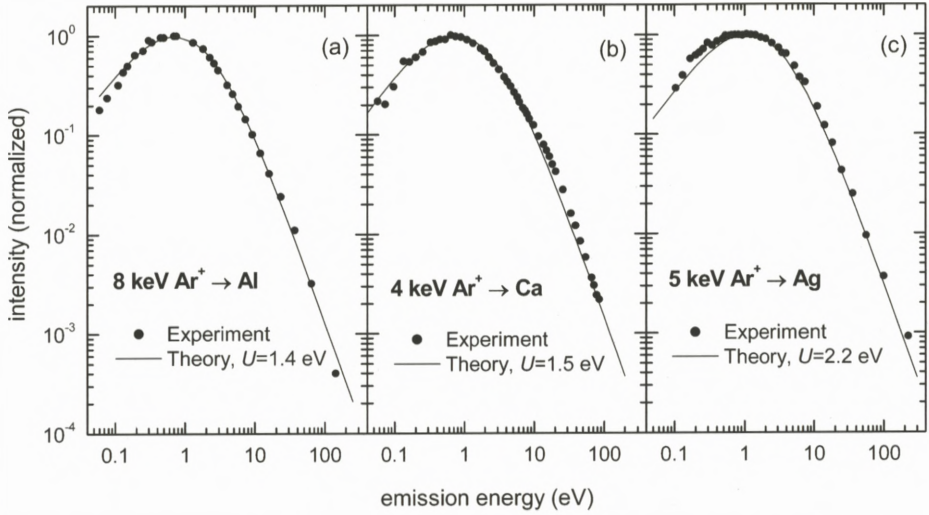


Figure 3. Emission energy distribution of neutral atoms sputtered from the respective elemental surface under bombardment with the indicated projectiles. The data were taken using multiphoton (a) or single photon (c) post-ionization with ToF mass spectrometry or Doppler shift laser fluorescence (b), respectively. The solid lines represent fits of Equation (1) using $m = 0$ and U as indicated. Reproduced from Gnaser (2006), with permission, original data Husinsky et al. (1993), Hansen et al. (1998) and Wahl and Wucher (1994).

elemental solid. It is seen that the measured surface binding energy may fall between 0.3 and 2 times the sublimation energy, depending on the target material and the employed experimental method. Moreover, even the data determined with the same method may exhibit discrepancies as large as a factor or two. The reason is presumably the large difficulty to assess (and eliminate) energy discrimination effects inherent in any of the experimental techniques used to determine the energy distribution. From the experience of the present author, any measured kinetic energy distribution published so far must be assumed to be influenced by such effects to some extent. While there is no debate about the principal shape of the energy distribution of sputtered atoms with a maximum at energies of the order of the sublimation energy and an asymptotic E^{-2} tail in the high energy regime, the actual most probable emission energy is not very accurately known. From an experimental point of view, it must therefore still be regarded as an open question whether the surface binding energy relevant in sputtering physics differs actually from the thermodynamical value of the sublimation energy or not.

For multicomponent targets, energy distributions of the same element sputtered from different compounds are generally found to differ (Gnaser, 2006). This is

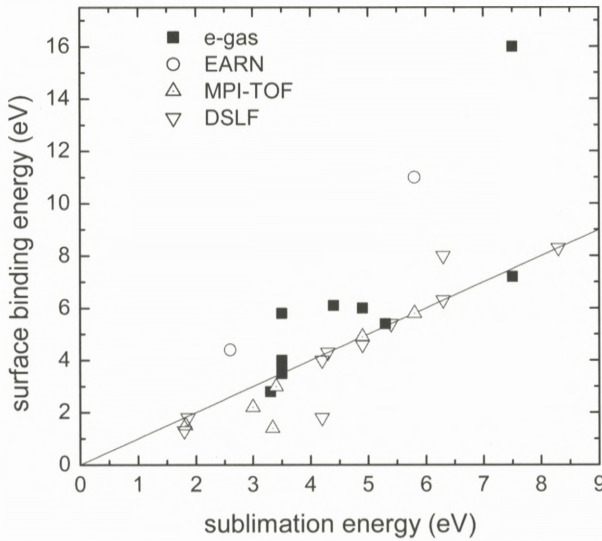


Figure 4. Surface binding energy U (Equation 1) determined for different target materials vs. sublimation energy U_s . The data have been extracted from experimental kinetic energy distributions of the respective sputtered neutral atoms employing different experimental methods as indicated (see text for meaning of abbreviations). Data taken from the compilation of Betz and Wien (1994) and Gnaser's recent review (2006) plus original data from Wahl and Wucher (1994), Ma et al. (1994) and Staudt et al. (2002) (Δ) and Baxter et al. (1986) and Garrison (1986) (\circ).

understandable, since it indicates a variation of the surface binding energy depending on the chemical environment of the ejected atom. In spite of the uncertainty regarding absolute values mentioned above, these effects can unambiguously be identified as long as the same method is used to determine all distributions. In this respect, measured energy spectra can provide valuable information about binding conditions at the bombarded surface.

2.3. ANGULAR DISTRIBUTIONS

In general, measured angular emission distributions of sputtered material are found to depend on the projectile energy. For amorphous or polycrystalline target materials and normal incidence, a variation from an under-cosine polar angle distribution at low energies to an over-cosine distribution in the limit of high impact energy is often observed. Under oblique incidence, these distributions are superimposed by a preferred off-normal ejection inclined towards the direction of specular projectile reflection. These findings are interpreted in terms of an incomplete randomization of the projectile momentum in the collision cascade.

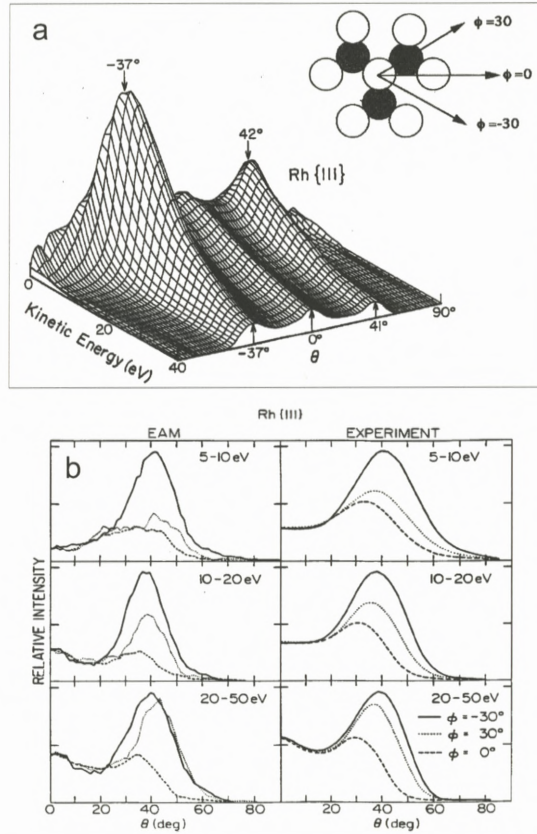


Figure 5. Polar emission angle distribution of neutral Rh atoms sputtered from a Rh(111) single crystal surface measured along two different azimuthal directions. For comparison, the same distributions calculated by molecular dynamics are shown (labeled "EAM"). Reproduced from Winograd et al. (1986) (a) and Maboudian et al. (1990) (b) with permission.

For single crystal targets, pronounced structure in the emission angle distributions is observed with preferred ejection along close packed lattice directions. These features are interpreted in terms of focusing collisions in combination with surface scattering of ejected particles. In particular, it has been shown early that the regular structure of only the uppermost two atomic layers may be sufficient to explain the observed distributions (Lehmann and Sigmund, 1966). By comparison with molecular dynamics computer simulations, even subtle details of the measured emission patterns can be reproduced. An example of this is shown in Figure 5, which depicts the energy resolved emission angle distribution of neutral

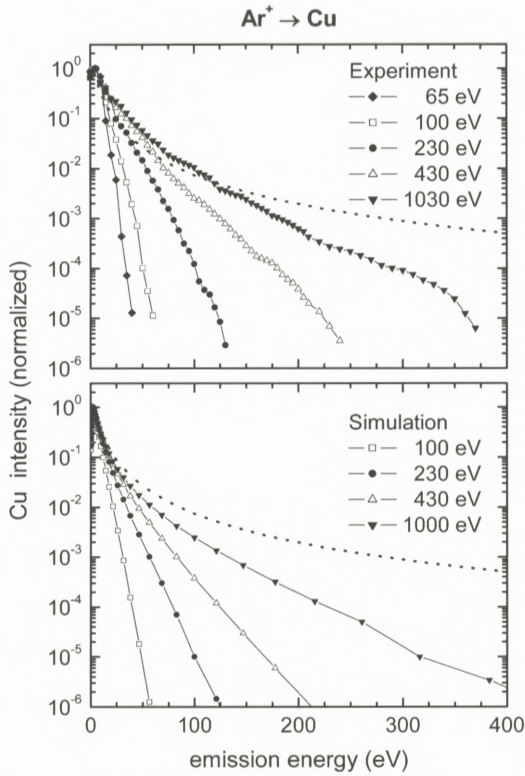


Figure 6. Emission angle integrated energy spectra of Cu atoms sputtered from copper under bombardment with normally incident Ar^+ ions. (a) Experimental data; b) computer simulation. Reproduced from Mousel et al. (1999) with permission.

Rh atoms sputtered along two different azimuth directions from a rhodium(111) surface under bombardment with normally incident 8-keV Ar^+ ions (Winograd et al., 1986). In conclusion, the angular distribution of atomic species ejected under linear cascade conditions appears to be well understood.

2.4. LOW ENERGY BOMBARDMENT

At impact energies significantly below 1 keV, deviations from the energy and angle distributions measured at higher energies are found.

First, the measured emission energy distribution appears to be truncated with a steeper than E^{-2} decay at high emission energies, leading to a quasi-exponential decay instead (Mousel et al., 1999). As shown in Figure 6, this experimental finding is reproduced by computer simulation (Mousel et al., 1999) and is, roughly

speaking, understood in terms of a limitation of the maximum energy transferrable to a recoil atom. Note, however, that there is a significant discrepancy between the exact shape of experimental and theoretical energy distributions depicted in Figure 6 particularly in the low emission energy regime. While the computer simulation agrees well with the prediction of linear cascade theory (Equation (1), dotted line), the experimental data do not. A close inspection of the data reveals that, for instance, the measured most probable emission energy is larger than theoretically predicted. This finding is in contrast with other data – taken with a very similar experimental method – which show a pronounced *reduction* of the most probable energy at low impact energies (Brizzolara and Cooper, 1988), again casting doubt about the accuracy of measured energy distributions at very low emission energies.

Second, a pronounced preferred ejection is observed at oblique emission angles, resulting in a heart-shaped polar angle distribution under normal incidence (Wehner and Rosenberg, 1960). This finding is indicative of single knock-on sputtering, i.e., the ejection of surface atoms after short sequences of only a few collisions. At the same time, a threshold behavior of the sputter yield is observed (see Urbassek, 2006, for more details). The angular distributions are of particular interest for multicomponent target materials. Here, the lighter component is often observed to be preferably ejected along the surface normal, while the heavier component is emitted under more oblique angles (Olson and Wehner, 1977) (see also Betz and Wehner, 1983; Sigmund and Lam, 1993, for a review). These effects, which are also predicted theoretically, are very important for applications of sputtering in thin film deposition and surface analysis. In general, they appear to be the more pronounced the lower the projectile impact energy. They are attributed to different types of collision sequences leading to the emission of different components (Betz and Wehner, 1983).

2.5. CLUSTER EMISSION

It is well known that the sputtered flux does not only contain atoms but also molecules and clusters. The formation and emission processes of such polyatomic species are much less completely understood than for sputtered atomic species. Partial sputter yields have been measured mostly for homonuclear clusters emitted from elemental surfaces or for oxide clusters emitted from oxides or oxidized surfaces. In the first case, the relative abundance of clusters vs. size or nuclearity n is generally found to roughly obey a power law (Wucher, 2002) (cf. also figure 11 in Urbassek, 2006)

$$Y(n) \propto n^{-\delta}, \quad (2)$$

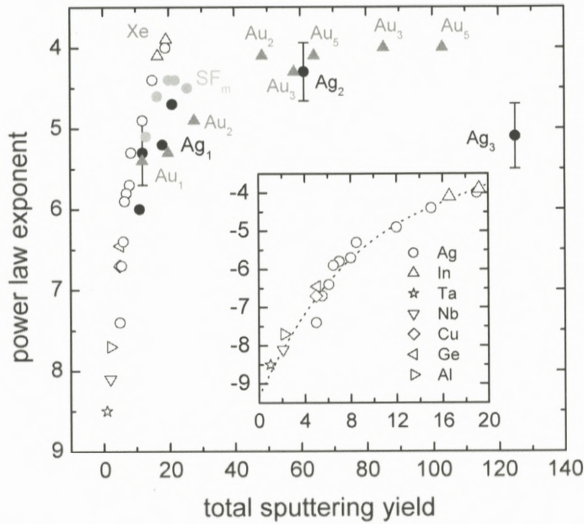


Figure 7. Power law exponent of sputtered cluster size abundance distribution (Equation 2) vs. total sputter yield for different projectiles, impact energies and target materials. The symbol shape codes the target material as indicated in the insert. Open symbols: data taken with rare gas projectile ions. Closed symbols: data taken with metal cluster projectiles as indicated.

with the exponent δ depending on the bombarding conditions and target material. In the linear cascade regime, the slope is found to be strongly correlated with the total sputter yield as illustrated in the insert of Figure 7. The theoretical implication of this observation is discussed in Urbassek (2006). For some favorable cases (e.g. bombardment of silver with 15-keV Xe^+ ; Staudt and Wucher, 2002a), it has been determined that the *majority* of sputtered atoms leaves the surface in a bound state, i.e., as part of a cluster. The kinetic energy distributions of emitted clusters exhibit similar most probable energies but a steeper asymptotic slope ($\propto E^{-\alpha}$) than the respective atomic species (Brizzolara and Cooper, 1989; Coon et al., 1993; Wahl and Wucher, 1994). Interestingly, the exponent α appears to be largely independent of cluster size. These findings are not yet fully understood and represent an open question in sputtering physics today.

For oxide clusters, a number of studies have been published regarding the relative abundance as a function of chemical composition of both the emitted cluster and the bombarded surface (Plog et al., 1977; Oechsner et al., 1978; Szymczak et al., 2006). Some of the work has been performed for secondary ions and will therefore not be discussed here. For sputtered neutrals, respective data have been accumulated using either electron impact or non-resonant laser post-ionization. Quite consistently, they show a reduction of atom yields and the occurrence of

cluster yields with varying oxygen content if the oxidation state of the surface is increased. Regarding the chemical composition of the sputtered cluster, yields are found to vary roughly according to simple statistical combinatorial models (Plog et al., 1977; Oechsner, 1985). The quantitative interpretation of these data has, however, been challenged by experiments utilizing resonant photoionization (Homolka et al., 1995; Goehlich, 2001) or laser induced fluorescence (Husinsky et al., 1984; Dullni, 1985) schemes to detect sputtered atoms in their electronic ground state. These experiments reveal an exceedingly low yield of ground state atomic species to be emitted from an oxide target. Similar observations have been made using non-resonant single photon post-ionization (Heinrich, 2002, unpublished), indicating that the low atom yield is not restricted to the electronic ground state alone. In addition, a very different emission energy distribution is measured than under non-resonant post-ionization conditions. These findings suggest that the *large majority* of the particle flux sputtered from an oxide surface may be emitted in form of clusters. This question has not been settled and represents an area of active research.

2.6. EXCITATION AND IONIZATION

Part of the sputtered material leaves the surface in electronically excited or ionized states. In general, the excitation probability tends to decrease with increasing excitation energy, and sizeable fractions are only found for atoms in low-lying states belonging to the ground state multiplet. The ion fraction is generally small, but may be large in exceptional cases of ionic or quasi-ionic solids (e.g. oxides). It forms the basis of Secondary Ion Mass Spectrometry and is discussed in great detail by Wittmaack (2006). Both excited and ionized fractions have been shown to depend strongly on the chemical environment of the emitted particle.

Excitation of sputtered material can manifest in different ways. For atomic species, *electronic* excitation has been studied extensively for short-lived states, since these are easy to detect by means of the emitted radiation (see Yu, 1991, for a review). However, a straightforward interpretation of the obtained data is not easy due to the interference of cascading transitions from higher-lying states. Metastable states have been investigated using laser spectrometric tools. Figure 8 shows a compilation of measured population partitions as a function of the excitation energy. It is seen that for a specific atom and state multiplet the data can be approximated by a Boltzmann distribution, but the resulting population “temperature” depends strongly on the investigated multiplet and appears to become larger with increasing excitation energy. Hence, the excitation mechanism is certainly not characterized by any sort of thermodynamic equilibrium.

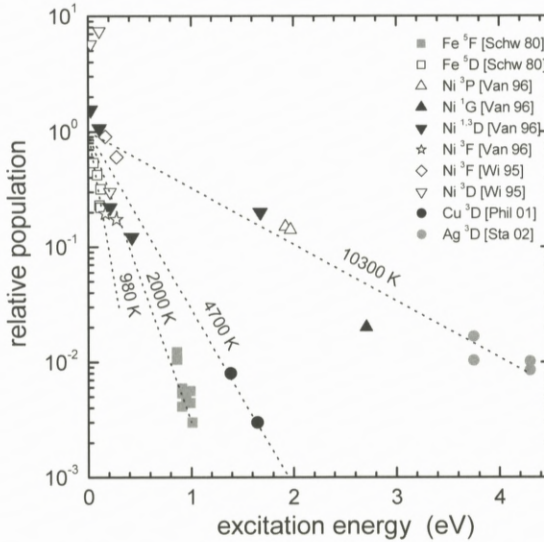


Figure 8. Population partition of metastable states of atoms sputtered from the respective elemental surface under bombardment with keV rare gas projectiles. Data taken from Schweer and Bay (1980), He et al. (1995), Vandeweert et al. (1995, 2001), Philipsen et al. (2000), Philipsen (2001) and Staudt et al. (2002).

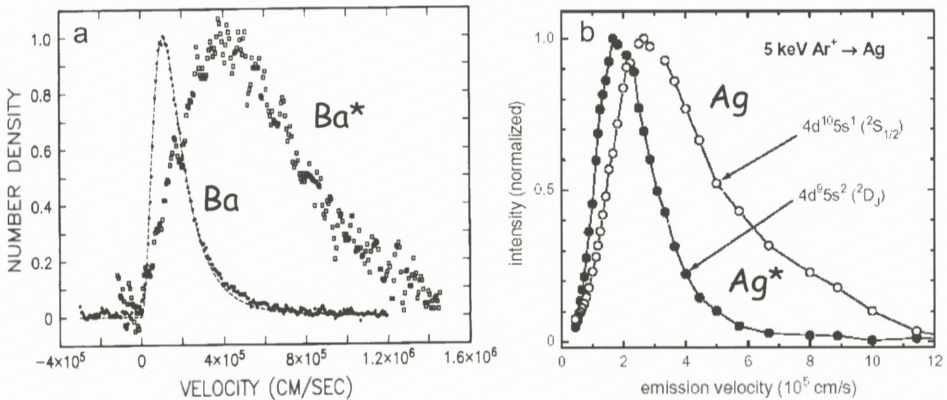


Figure 9. Emission velocity distribution of metastable Ba* (a) and Ag* (b) atoms sputtered from the respective clean elemental surfaces under in comparison with that of ground state Ba and Ag, respectively. Reproduced from Yu et al. (1982) (a) and Staudt et al. (2002) (b) with permission.

The kinetic energy distributions of atoms ejected in excited states are often found to differ from those emitted in the electronic ground state. Examples are depicted in Figure 9, which shows the distributions measured for Ba* (Grischkowsky et al., 1983) and Ag* (Berthold and Wucher, 1997; Staudt et al., 2002) in comparison with those of the respective ground state atoms. The data for barium appear typical for a relatively large set of experiments performed for other metal targets as well (see Garrison et al., 1998, for a review), always revealing a broader distribution for the excited state. This finding has been interpreted in terms of resonant electron transfer between the outgoing atom and the (electronically undisturbed) solid surface (Craig et al., 1986; Vandeweert et al., 2001). Alternatively, it has been suggested that the sputtered atoms carry an excitation signature which “remembers” the electronic band structure in the solid (He et al., 1995). The data depicted for silver, on the other hand, represent an exceptional case where the excited atoms are emitted with *lower* kinetic energy than those in the ground state. Similar findings have been obtained for Cu* as well (Philipsen, 2001). These observations are not understandable by either band structure arguments or resonant electron transfer between single electron states. This is corroborated by the relatively high population of the two Ag* states (Figure 8), since these states are energetically located well above the Fermi level and are therefore outside the excitation window generally thought to be accessible by such processes. A sound interpretation of these observations is still lacking. It has been attempted to interpret the experimental results via a time dependence of the collision induced electronic excitation processes within the solid, leading to different ejection times of excited and ground state atoms (Sroubek et al., 2003). However, the picture is far from being complete and represents an area of active research.

Besides electronic excitation, molecular species emitted from the surface may be *ro-vibrationally* excited. For diatomic molecules, this phenomenon has been investigated by laser spectroscopy (Fayet et al., 1986; De Jonge et al., 1986; Wucher, 1994). In one case, these experiments have been extended to larger clusters as well (Staudt et al., 2001). It was found that sputtered clusters are internally hot, exhibiting vibration temperatures which may be as high as several thousand Kelvin. Molecular dynamics studies have revealed that the clusters initially leave the surface with internal energies of the order of 1 eV per constituent atom (Lindenblatt et al., 2001). These “nascent” clusters are unstable and therefore decompose by unimolecular fragmentation during their flight away from the surface, leading to either stable or metastable “final” fragments which are then detectable by experiment. While MD reveals that this decomposition mainly proceeds on a picosecond time scale, the late stages of such fragmentation chains may be observed on a nano- or microsecond time scale tractable by experiment. Unfortunately, most of

these experiments have been performed for molecular secondary ions (Begemann et al., 1986; Dzhemilev et al., 1991; Delcorte et al., 2005). The available data reveal, however, clear evidence for the occurrence of metastable fragmentation in vacuum.

3. The Spike Regime

A general characteristic of a spike is that the condition of linearity breaks down and collisions between moving particles become important. It is important to note that – due to the statistical nature of the sputtering process – spikes can occur for specific impacts even under conditions where the average event falls well into the linear cascade regime. As outlined in Andersen's review (1993), spikes form if the energy per target atom deposited by the projectile impact becomes comparable with the binding energy in the solid. One possible scenario involves the impact of sufficiently heavy atomic projectiles onto a sufficiently weakly bound target. A second scenario which has been actively studied during the recent years is by impact of cluster projectiles. In the following, particular emphasis will be put on this latter aspect, since it bears great implication for applications of the sputtering process.

3.1. YIELDS

In many cases, cluster bombardment leads to strong enhancements of the sputter yield which are nonlinear in the sense that the yield observed under cluster impact is larger than that observed for the constituents impinging independently at the same velocity. For di- and triatomic projectiles, examples of this effect have been demonstrated many years ago (Andersen and Bay, 1974). More recently, the spectrum of available projectile size has been dramatically extended, and giant sputter yields of thousands of atoms per projectile impact have been measured, for instance, under bombardment of gold and silver with Au_n^+ cluster ions ($n = 1-13$) (Bouneau et al., 2002). The simple minded picture behind this observation is that the projectile cluster disintegrates upon impact, leaving each constituent with a reduced kinetic energy (corresponding to the same impact velocity as the original cluster) which is then deposited relatively close to the surface. As a consequence, the energy density condition for nonlinearity is easily fulfilled in the near-surface region and spikes develop even for moderate impact energies.

It should be noted at this point that yield enhancements observed under cluster bombardment are not necessarily nonlinear. In fact, one has to be careful with the language in this respect. Analyzing, for instance, data measured under 10-keV impact of SF_6^+ onto metallic surfaces, it was shown that the observed yield increase

with respect to Xe^+ projectiles (of roughly the same mass and *kinetic energy*) can be fully understood by a linear superposition of effects induced individually by the projectile constituents (Ghalab and Wucher, 2004). In this case, the large enhancement observed for corresponding secondary ion yields are largely attributable to an increase of the ion fraction, presumably induced by the incorporation of fluorine into the surface.

In other cases, on the other hand, strong nonlinearity is observed. This is particularly true for heavy projectiles like Au_m (Bouneau et al., 2002), larger clusters like C_{60} (Winograd, 2005), Au_{400} (Tempez et al., 2004), Ar_{1000} (Matsuo et al., 1997) or even more massive clusters containing about 10^6 glycerol molecules (Mahoney et al., 1991). Particularly the sizeable yields observed in the two latter cases manifest an infinite nonlinear enhancement in the sense defined above, since each Ar or glycerol constituent would impinge with an impact energy of only several eV, i.e., certainly below the threshold for sputtering, and therefore the added yields induced by the cluster constituents impinging independently would be zero. For large projectiles, collective emission processes must therefore prevail.

3.2. ENERGY DISTRIBUTIONS

Models of emission scenarios under spike conditions are summarized in Urbassek (2006). The experimental yield data have mainly been analyzed in terms of thermodynamical models involving either thermal evaporation or hydrodynamic expansion mechanisms. Some of these models make a prediction with respect to the emission energy distribution of the sputtered material. Corresponding reliable experimental data, however, have become available only recently. As an example, the velocity distributions of In atoms and In_2 dimers sputtered from polycrystalline indium under bombardment with Au_m^- projectile ions are depicted in Figure 10 (Samartsev and Wucher, 2006a). Although not shown, the spectra measured under Au_3 bombardment are practically identical to that depicted for Au_2 projectiles (Samartsev and Wucher, 2005). It is seen that cluster bombardment leads to a pronounced contribution of low-energy sputtered material, which is incompatible with the prediction of linear cascade theory (solid line in Figure 10) and represents a clear signature of the spike emission process. Analyzing the exact form of this contribution, one finds reasonable agreement with a gas flow model involving a “phase explosion” of supercritically heated material (cf. Urbassek, 2006), while the measured spectrum cannot be explained by a thermal desorption mechanism (Samartsev and Wucher, 2005). In addition, the velocity distributions of sputtered atoms and dimers are found to be quite similar (see Figure 10). The same observation has been made for other metals under bombardment with C_{60} projectiles (Sun et al., 2005). In contrast, energy spectra of monomers

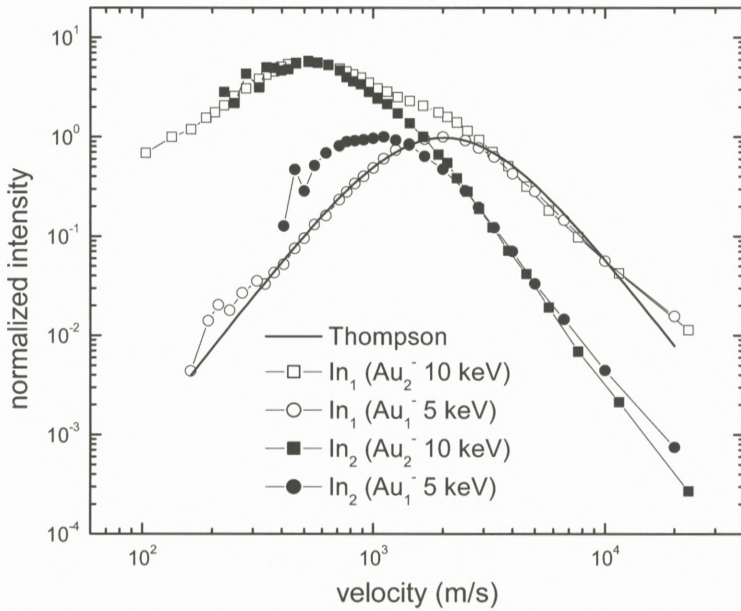


Figure 10. Emission velocity distribution of In atoms and In_2 dimers sputtered from polycrystalline Indium under bombardment with 5-keV/atom Au_m^- projectiles. Reproduced from Samartsev and Wucher (2006a) with permission.

and dimers are found to be distinctly different under linear cascade sputtering conditions (Brizzolara and Cooper, 1989; Coon et al., 1993). Unfortunately, no experimental data on the velocity distributions of larger neutral clusters produced under polyatomic projectile bombardment are available yet. Measurements of the corresponding secondary ions (Morozov and Rasulev, 2004) suggest that this similarity may continue towards larger sputtered molecular species as well. These findings would be consistent with a hydrodynamical spike emission process.

3.3. CLUSTER EMISSION

In view of the large sputter yields from spikes, one may ask about the magnitude of cluster emission in this regime of sputtering. If the scaling of cluster abundance with total sputter yield observed in the linear cascade regime was continued, one would expect the flux of particles sputtered from spikes to be largely dominated by clusters. Experiment, however, shows that this is not the case. As depicted in Figure 7, the power law exponent characterizing the cluster abundance distribution (Equation 2) becomes roughly constant for yields above approximately 20

atoms/projectile. Interestingly, it has been suggested that a yield value of this order should separate the linear cascade from the spike regimes of sputtering (Sigmund and Claussen, 1981; Andersen, 1993). Hence, spikes appear to produce cluster emission at a rate which is largely independent of the total sputter yield. Conversely, one example has been published where *less* cluster emission was observed under bombardment with *larger* clusters of *higher* impact energy, leading to *larger* sputter yield (Heinrich and Wucher, 2003) (cf. the data for 7-keV/atom Ag_n^+ projectiles in Figure 7). This observation has been interpreted in terms of the average energy deposited in the spike volume. As shown by computer simulation (Colla and Urbassek, 1996), optimum conditions for cluster emission prevail if the deposited energy density roughly equals the binding energy per atom. A crude estimate shows that this condition is approximately fulfilled under bombardment of silver with 14-keV Ag_2 , while the optimum energy density is exceeded for 21-keV Ag_3 impact, and therefore the abundance of clusters in the sputtered flux is diminished.

In this light, the data set displayed in Figure 7 can be interpreted as follows. In the spike regime, cluster emission appears to be largely governed by the deposited energy density. Optimum conditions are found if the deposited energy equals the binding energy of atoms or molecules within the solid. In contrast, the total sputter yield seems to scale with the total energy of the impinging projectile (Urbassek, 2006), and no apparent correlation is found between cluster abundance and total sputter yield. This is different in the linear cascade regime. All published MD simulations show that (large) cluster emission is always connected to specific events where spikes are formed. This appears to be true even if the average event produced under the prevailing bombardment conditions clearly falls into the linear cascade regime. In this case, the observed scaling with total sputter yield simply reflects the probability for spike events to occur, which of course increases with increasing yield. As a consequence, one may conclude that the emission of clusters larger than dimers in sputtering is largely a spike phenomenon rather than a collision cascade effect.

3.4. IONIZATION AND EXCITATION

As outlined above, spikes are associated with large deposited energy density, leading to drastic enhancements of sputter yields. A very pronounced effect of electronic excitation in this scenario is that of a sink of kinetic energy, acting to effectively cool the spike in metallic targets (Flynn and Averbach, 1988). One may of course ask if the excitation degree within the spike volume, as manifested, for instance, by electron emission yields or excitation/ionization probabilities of sputtered particles, is enhanced as well. The available experimental data suggest that

this is not the case. Although several publications have advocated the idea of enhanced secondary ion formation under cluster bombardment (Belykh et al., 2002), recent measurements of ionization probabilities of In atoms sputtered under Au_n cluster impact reveal no change as a function of projectile nuclearity n (Samartsev and Wucher, 2006b). As of today, no data exist regarding excitation probabilities of sputtered material under cluster impact. Experiments on ion induced electron emission even indicate a “sub-linear” effect, i.e., the electron yield per projectile constituent atom observed under Au_n cluster bombardment of insulating target materials is found to decrease with increasing n (Baudin et al., 1998). To the best of our knowledge, corresponding data for metal targets are not yet available, and the question of electronic excitation under cluster bombardment is a topic of active research.

3.5. MOLECULAR SOLIDS

Probably the largest advantage of cluster vs. atomic projectiles is observed for molecular solids. For this class of target material, exceedingly large sputter yields are found quite regularly. As an example, about 2700 H_2O molecule equivalents are sputtered from a water ice surface bombarded with 20-keV C_{60} projectiles (Wucher et al., 2004). In comparison, the largest yield value measured for any atomic projectile amounts to about 100 molecule equivalents per projectile impact (Baragiola et al., 2003). Similar observations are made for organic samples. For instance, a thick overlayer of trehalose ($C_{12}H_{22}O_{11} \times 2H_2O$, a sugar) on, say, a Si substrate, exhibits a yield of about 300 molecule equivalents under the same bombardment conditions (Cheng et al., 2006). These values reveal that about 10^4 atoms are sputtered per cluster projectile impact.

This finding has generated large interest in the use of cluster projectiles in surface analysis. In this field of applications, one central role of the sputtering process is to generate the signal detected in mass spectrometric techniques like SIMS. It is obvious that yield enhancements of an order of magnitude will increase the detection sensitivity accordingly. Moreover, static SIMS spectra of molecular samples often reveal less fragmentation and therefore a more complete preservation of the molecular information for cluster compared to isoenergetic atomic projectiles (see Wucher, 2006, for a review). The largest advantage, however, is found in sputter depth profiling applications, where the sputtering process is utilized as a micro-sectioning tool eroding the surface. For decades, it has been common wisdom that this method is virtually impossible to apply to molecular solids, since the ion bombardment inevitably leads to the accumulation of chemical damage which ultimately destroys the molecular integrity of the investigated surface. With the advent of ion sources delivering cluster projectile beams of sufficient quality to

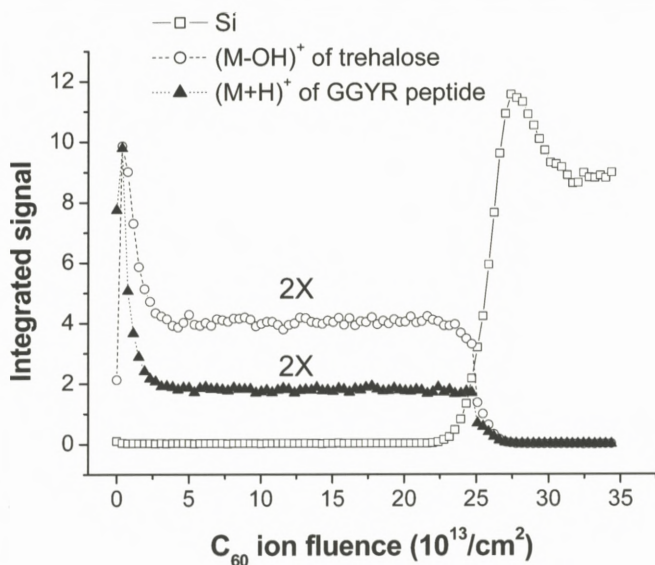


Figure 11. SIMS sputter depth profile of a 300-nm Trehalose overlayer doped with GGYR peptide on a Si substrate. The data were obtained using a 20-keV C_{60}^+ projectile ion beam for sputter erosion and data acquisition. Reproduced from Cheng et al. (2005) with permission.

be employed for surface analysis, however, this notion has changed dramatically. Using cluster ion beams like Au_3^+ , Bi_3^+ or C_{60}^+ , it was recently demonstrated that sputter depth profiles of organic overlayers may be acquired without accumulation of chemical damage, thereby preserving the molecular information until complete removal of the entire overlayer. An example of such an application is shown in Figure 11, where a 300-nm overlayer of trehalose doped with a GGYR peptide on a Si substrate was subjected to 20-keV C_{60}^+ ion bombardment for sputter erosion and mass spectrometric characterization of the receding surface. The SIMS signals observed for the molecular ions of the trehalose matrix and the peptide dopant, respectively, are preserved throughout the removal of the entire overlayer, until they drop sharply at the interface to the underlying Si substrate. While a similar result is obtained under Au_3^+ bombardment, it is impossible to acquire such a depth profile using atomic projectiles of any mass and impact energy. The reason is seen from a simple model describing the erosion dynamics (Cheng et al., 2006); the large sputter yield obtained under cluster bombardment ensures that most of the debris produced by ion induced chemical damage is removed during the same impact event, exposing intact molecules to analysis at the eroded surface.

4. Conclusions

Many of the experimental observations on sputtering in the linear cascade regime have been properly understood. From the perspective of an experimentalist, the prevailing emission mechanisms are clear, and observables like sputter yields or energy and angular distributions of the sputtered material can be predicted with reasonable accuracy. There are, however, a few open questions which remain to be unsolved even after many years of investigation. These are

- What is the exact nature of the surface binding energy relevant in sputtering?
- Why are the cluster abundance distributions power laws and what determines the power law exponent?
- What are the physical mechanisms behind the electronic excitation of sputtered particles?

In the spike regime, things are less clear. From the presently available data, it is obvious that mesoscale hydrodynamic emission mechanisms must be operative instead of the often assumed “thermal spikes”. Material is ejected at very large yields and with lower average kinetic energy than in the linear cascade regime. Moreover, clusters and atoms are emitted with comparable velocity distributions. Ionization of the sputtered material does not seem to be enhanced very much. So far, these observations have not been well understood, and it is certainly not possible for an experimentalist to make a reasonable estimate of quantities like yields, energy or angle distributions or ion fractions on the basis of the published models. According to my understanding, the main open questions in this regime of sputtering are

- How does the sputter yield scale with experimental parameters like energy, mass and nuclearity of the impinging projectiles as well as the binding energy of the bombarded solid?
- Why can measured sputter yields be reasonably well interpreted in terms of thermal spike models, but the resulting spike “temperatures” are (i) much larger than the critical temperature of the solid material and (ii) incompatible with measured energy spectra?
- What is the angular distribution of sputtered material and how is it influenced by experimental conditions?
- Is there a common physical basis behind spike sputtering and laser ablation?
- Is there an enhanced probability of electronic excitation or ionization of sputtered species under spike conditions?

- How does the spike mechanism prevent the accumulation of damage in the limit of large projectile fluence?
- What is the depth of origin of sputtered material and how does it relate to depth resolution achievable in sputter depth profiling applications?

Many of these questions are currently actively investigated. This is particularly true for the spike sputtering regime, since the advent of commercially available cluster ion sources has sparked renewed interest in the application of polyatomic projectiles in thin film technology and surface analysis. Particularly for the latter, cluster bombardment may constitute a major breakthrough with respect to the three-dimensional characterization of organic and biological systems.

References

- Andersen H.H. (1993): Nonlinear effects in collisional sputtering under cluster impact. In: Sigmund P. (Ed.), *Fundamental Processes in Sputtering of Atoms and Molecules (SPUT 92)*. Det Kongelige Danske Videnskabernes Selskab, Copenhagen, pp 127–153
- Andersen H.H. and Bay H.L. (1974): Nonlinear effects in heavy-ion sputtering. *J Appl Phys* **45**, 953–954
- Andersen H.H. and Bay H.L. (1981): Sputtering yield measurements. In: Behrisch R. (Ed.), *Sputtering by Particle Bombardment*, Vol. 1. Springer, Berlin, pp 145–218
- Bach H. (1970): Determination of bond energy of silica glass by means of ion sputtering investigations. *Nucl Instrum Meth* **84**, 4–12
- Bach H., Kitzmann I. and Schröder H. (1974): Sputtering yields and specific energy losses of Ar(sup +) ions with energies from 5 to 30 KeV at SiO(sub 2). *Radiat Eff* **21**, 31–36
- Baragiola R.A., Vidal R.A., Svendsen W., Schou J., Shi M., Bahr D.A. and Atteberry C.L. (2003): Sputtering of water ice. *Nucl Instrum Meth B* **209**, 294–303
- Baudin K., Parilis E.S., Blankenship J.F., van Stipdonk M.J. and Schweikert E.A. (1998): Sublinear effect in light emission from cesium iodide bombarded by keV polyatomic projectiles. *Nucl Instrum Meth B* **134**, 352–359
- Baxter J.P., Singh J., Schick G.A., Kobrin P.H. and Winograd N. (1986): Energy and angle-resolved studies of neutrals desorbed from ion bombarded polycrystalline metal surfaces. *Nucl Instrum Meth B* **17**, 300–304
- Begemann W., Meiwes-Broer K.H. and Lutz H.O. (1986): Unimolecular decomposition of sputtered Al/sub n/sup +/, Cu/sub n/sup +/, and Si/sub n/sup +/ clusters. *Phys Rev Lett* **56**, 2248–2251
- Belykh S.F., Palitsin V.V., Adriaens A. and Adams F. (2002): Effect of projectile parameters on charge state formation of sputtered atoms. *Phys Rev B* **66**, 195309-1–195309-10
- Berthold W. and Wucher A. (1997): Energy- and angle-dependent excitation probability of sputtered metastable silver atoms. *Phys Rev B* **56**, 4251–4260
- Betz G. (1987): Electronic excitation in sputtered atoms and the oxygen effect. *Nucl Instrum Meth B* **27**, 104–118
- Betz G. and Wehner G.K. (1983): Sputtering of multicomponent materials. In: Behrisch R. (Ed.), *Sputtering by Particle Bombardment*, Vol. 2. Springer, Heidelberg, pp 11–90

- Betz G. and Wien K. (1994): Energy and angular distributions of sputtered particles. *Int J Mass Spectrom Ion Proc* **140**, 1–110
- Bouneau S., Brunelle A., Della-Negra S., Depauw J., Jacquet D., Le Beyec Y., Pautrat M., Fallavier M., Poizat J.C. and Andersen H.H. (2002): Very large gold and silver sputtering yields induced by keV to MeV energy Au/sub *n*/ clusters (*n* = 1–13). *Phys Rev B* **65**, 144106–144108
- Brizzolara R.A. and Cooper C.B. (1989): Measurements of energy distributions and yields of neutral Cu/sub 2/ and Cu/sub 3/ species sputtered from Cu by low energy Ar/sup +/- ions. *Nucl Instrum Meth B* **43**, 136–145
- Brizzolara R.A., Cooper C.B. and Olson T.K. (1988): Energy distributions of neutral atoms sputtered by very low energy heavy ions. *Nucl Instrum Meth B* **35**, 36–42
- Cheng J. and Winograd N. (2005): Depth profiling of peptide films with TOF-SIMS and a C-60 probe. *Anal Chem* **77**, 3651–3659
- Cheng J., Wucher A. and Winograd N. (2006): Molecular depth profiling with cluster ion beams. *J Phys Chem B* **110**, 8329–8336
- Colla T.J. and Urbassek H.M. (1996): Effect of energy density on cluster formation from energized metals. *Comp Mater Sci* **6**, 7–14
- Coon S.R., Calaway W.F., Pellin M.J. and White J.M. (1993): New findings on the sputtering of neutral metal clusters. *Surf Sci* **298**, 161–172
- Craig B.I., Baxter J.P., Singh J., Schick G.A., Kobrin P.H., Garrison B.J. and Winograd N. (1986): Deexcitation model for sputtered excitation neutral atoms. *Phys Rev Lett* **57**, 1351–1354
- Davidse P.D. and Maissel L.I. (1967): Equivalent dc sputtering yields of insulators. *J Vac Sci Technol* **4**, 33–36
- De Jonge R., Baller T., Tenner M.G., de Vries A.E. and Snowdon K.J. (1986): Rotational, vibrational and translational energy distributions of sputtered S/sub 2/ molecules. *Europhys Lett* **2**, 449–453
- Delcorte A., Poleunis C. and Bertrand P. (2005): Energy distributions of atomic and molecular ions sputtered by C₆₀⁺ projectiles. *Appl Surf Sci* **252**, 6542–6546
- Dullni E. (1985): Laser fluorescence measurements of the flux density of titanium sputtered from an oxygen covered surface. *Appl Phys A* **38**, 131–138
- Dzhemilev N.Kh., Goldenberg A.M., Vervovkin I.V. and Verkhoturov S.V. (1991): The influence of unimolecular cluster decompositions in the nanosecond time range on the secondary ion mass spectrum of tantalum. *Int J Mass Spectrom Ion Proc* **107**, R19–R25
- Fayet P., Wolf J.P. and Woeste L. (1986): Temperature measurement of sputtered metal dimers. *Phys Rev B* **33**, 6792–6797
- Flynn C.P. and Averback R.S. (1988): Electron-phonon interactions in energetic displacement cascades. *Phys Rev B* **38**, 7118–7120
- Garrison B.J. (1986): Energy distributions of atoms sputtered from polycrystalline surfaces. *Nucl Instrum Meth B* **17**, 305–308
- Garrison B.J., Winograd N., Chatterjee R., Postawa Z., Wucher A., Vandeweert E., Lievens P., Philipsen V. and Silverans R.E. (1998): Sputtering of atoms in fine structure states: A probe of excitation and de-excitation events. *Rapid Commun Mass Sp* **12**, 1266–1272
- Ghalab S. and Wucher A. (2004): Cluster formation at metal surfaces under bombardment with SF(sub *m*)(sup +) (*m* = 1, . . . , 5) and Ar(sup +) projectiles. *Nucl Instrum Meth B* **226**, 264–273
- Gnaser H. (2006): Energy and angular distributions of sputtered species. In: Behrisch R. (Ed.), *Sputtering by Particle Bombardment*, Vol. 4. Springer, pp 1–92, to be published

- Goehlich A. (2001): Investigation of time-of-flight and energy distributions of atoms and molecules sputtered from oxygen-covered metal surfaces by laser-aided techniques. *Appl Phys A* **72**, 523–529
- Grischkowsky D., Yu M.L. and Balant A.C. (1983): The effect of oxygen on the sputtering of metastable atoms and ions from Ba metal. *Surf Sci* **127**, 315–330
- Hansen C.S., Calaway W.F., King B.V. and Pellin M.J. (1998): Energy and yield distributions of calcium atoms and clusters undergoing 4 keV Ar/sup +/- ion bombardment. *Surf Sci* **398**, 211–220
- He C., Postawa Z., Rosencrance S.W., Chatterjee R., Garrison B.J. and Winograd N. (1995): Band structure effects in ejection of Ni atoms in fine structure states. *Phys Rev Lett* **75**, 3950–3953
- Heinrich R. and Wucher A. (2003): Projectile size effects on cluster formation in sputtering. *Nucl Instrum Meth B* **207**, 136–144
- Homolka P., Husinsky W., Nicolussi G., Betz G. and Li X. (1995): Matrix effects of secondary neutrals: laser postionization investigations of particles sputtered from clean and oxidized metals. *Phys Rev B* **51**, 4665–4667
- Husinsky W., Betz G. and Girgis I. (1984): Ground state and excited state sputtering Doppler-shift laser-fluorescence studies of Cr and Ca targets. *J Vac Sci Technol* **2**, 698–701
- Husinsky W., Nicolussi G. and Betz G. (1993): Energy-distributions of sputtered metal Al-clusters. *Nucl Instrum Meth B* **82**, 323–328
- Jorgenson G.V. and Wehner G.K. (1965): Sputtering studies of insulators by means of Langmuir probes. *J Appl Phys* **36**, 2672–2675
- Kobrin P.H., Schick G.A., Baxter J.P. and Winograd N. (1986): Detector for measuring energy- and angle-resolved neutral-particle (EARN) distributions for material desorbed from bombarded surface. *Rev Sci Instr* **57**, 1354–1362
- Lehmann C. and Sigmund P. (1966): On the mechanism of sputtering. *Phys Status Solidi* **16**, 407–511
- Lindenblatt M., Heinrich R., Wucher A. and Garrison B.J. (2001): Self-sputtering of silver by mono- and polyatomic projectiles: A molecular dynamics investigation. *J Chem Phys* **115**, 8643–8654
- Ma Z., Calaway W.F., Pellin M.J. and Nagy-Felsobuki E.I. (1994): Kinetic energy distributions of sputtered indium atoms and clusters. *Nucl Instrum Meth B* **94**, 197–202
- Maboudian R., Postawa Z., El Maazawi M., Garrison B.J. and Winograd N. (1990): Angular distribution of Rh atoms desorbed from ion-bombarded Rh(100): Effect of local environment. *Phys Rev B* **42**, 7311–7316
- Mahoney J.F., Perel J., Ruatta S.A., Martino P.A., Husain S. and Lee T.D. (1991): Massive cluster impact mass spectrometry: A new desorption method for the analysis of large biomolecules. *Rapid Commun Mass Sp* **5**, 441
- Matsunami N., Yamamura Y., Itikawa Y., Itoh N., Kazumata Y., Miyagawa S., Morita K., Shimizu R. and Tawara H. (1984): Energy dependence of the ion-induced sputtering yields of monatomic solids. *At Data Nucl Data Tables* **31**, 1–80
- Matsuo J., Toyoda N., Akizuki M. and Yamada I. (1997): Sputtering of elemental metals by Ar cluster ions. *Nucl Instrum Meth B* **121**, 459–463
- Morozov S.N. and Rasulev U.K. (2004): Non-additive effects in secondary-ion emission from V, Nb and Ta under gold-cluster bombardment. *Appl Surf Sci* **231–232**, 78–81
- Mousel T., Eckstein W. and Gnaser H. (1999): Energy spectra of sputtered species under sub-keV ion bombardment: Experiments and computer simulations. *Nucl Instrum Meth B* **152**, 36–48

- Oechsner H. (1985): Formation of sputtered Molecules. In: Popovic M.M. et al. (Eds), *The Physics of Ionized Gases*. World Scientific, Singapore, pp 571–598
- Oechsner H., Schoof H. and Stumpe E. (1978): Sputtering of Ta₂O₅ by Ar⁺ ions at energies below 1 keV. *Surf Sci* **76**, 343–354
- Olson R.R. and Wehner G.K. (1977): Composition variations as a function of ejection angle in sputtering of alloys. *J Vac Sci Technol.* **14**, 319–321
- Philipsen V. (2001): Resonant electron transfer during sputtering of metals studied by resonant laser ionization. PhD Thesis, KU Leuven.
- Philipsen V., Bastiaansen J., Lievens P., Vandeweert E. and Silverans R.E. (2000): Resonant electron transfer in the emission of ion-beam sputtered metal atoms studied by double resonance laser ionization. *Vacuum* **56**, 269–274
- Plog C., Wiedmann L. and Benninghoven A. (1977): Empirical formula for the calculation of secondary ion yields from oxidized metal surfaces and metal oxides. *Surf Sci* **67**, 565–580
- Samartsev A. and Wucher A. (2005): Sputtering of indium using Au_m projectiles: Transition from linear cascade to spike regime. *Phys Rev B* **72**, 115417-1–10
- Samartsev A. and Wucher A. (2006a): Kinetic energy distributions of neutral In and In₂ sputtered by polyatomic ion bombardment 2704. *Appl Surf Sci* **252**, 6470–6473
- Samartsev A. and Wucher A. (2006b): Mass spectra and ionization probabilities of Indium species sputtered by atomic and polyatomic ion bombardment. *Appl Surf Sci* **252**, 6474–6477
- Schweer B. and Bay H.L. (1980): Measurements of the population distribution of sputtered Fe-atoms with laser induced fluorescence spectroscopy. In: Fourth International Conference on Solid Surfaces and The Third European Conference on Surface Science, Cannes, 20–26.09.1980 II, pp 721–1448
- Sigmund P. (1969): Theory of sputtering. I. Sputtering yield of amorphous and polycrystalline targets. *Phys Rev* **184**, 383–416
- Sigmund P. (1981): Sputtering by ion bombardment: Theoretical concepts. In: Behrisch R. (Ed.), *Sputtering by Particle Bombardment*, Vol. I. Springer, Berlin, pp 9–72
- Sigmund P. and Claussen C. (1981): Sputtering from elastic-collision spikes in heavy-ion-bombarded metals. *J Appl Phys* **52**, 990–993
- Sigmund P. and Lam N.Q. (1993): Alloy and isotope sputtering. In: Sigmund P. (Ed.), *Fundamental Processes in Sputtering of Atoms and Molecules (SPUT 92)*, Det Kongelige Danske Videnskabernes Selskab, Copenhagen, pp 255–350
- Sroubek Z., Sroubek F., Wucher A. and Yarmoff J.A. (2003): Formation of excited Ag atoms in sputtering of silver. *Phys Rev B* **68**, 115426-1–115426-5
- Staudt C. and Wucher A. (2002): Generation of large indium clusters by sputtering. *Phys Rev B* **66**, 075419-1–075419-12
- Staudt C., Wucher A., Neukermans S., Janssens E., Vanhoutte F., Vandeweert E., Silverans R.E. and Lievens P. (2001): Internal excitation of sputtered neutral indium clusters. *Nucl Instrum Meth B* **193**, 787–793
- Staudt C., Wucher A., Bastiaansen J., Philipsen V., Vandeweert E., Lievens P., Silverans R.E. and Sroubek Z. (2002): Sputtering of Ag atoms into metastable excited states. *Phys Rev B* **66**, 085415-1–085415-12
- Sun S., Szakal C., Winograd N. and Wucher A. (2005): Energetic ion bombardment of Ag surfaces with C₆₀⁺ and Ga⁺ projectiles. *J Am Soc Mass Spectrom* **16**, 1677–1687

- Szymczak W., Menzel N., Kreyling W.G. and Wittmaack K. (2006): TOF-SIMS characterisation of spark-generated nanoparticles made from pairs of Ir-Ir and Ir-C electrodes. *Int J Mass Spectrom* **254**, 70–84
- Tempez A., Schultz J.A., Della-Negra S., Depauw J., Jacquet D., Novikov A., Le Beyec Y., Pautrat M., Caroff M., Ugarov M., Bensaoula H., Gonin M., Fuhrer K. and Woods A. (2004): Orthogonal time-of-flight secondary ion mass spectrometric analysis of peptides using large gold clusters as primary ions. *Rapid Commun Mass Sp* **18**, 371
- Thompson M.W. (1968): On the energy spectrum of sputtered Au. *Philos Mag* **18**, 377
- Tu Y.Y., Chuang T.J. and Winters H.F. (1980): The chemical sputtering of fluorinated silicon. In: Varga P., Betz G. and Viehböck F.P. (Eds), *Proc. Symp. on Sputtering*, Perchtoldsdorf, 28–30.04.1980, pp 337–389
- Urbassek H.M. (2006): Sputter theory. *Mat Fys Medd Dan Vid Selsk* **52**, 433–463
- Vandeweert E., Thoen P., Qamhieh Z.N., Lievens P. and Silverans R.E. (1995): The electronic excitation of atoms in atomization processes studied by resonance ionization mass spectrometry. *AIP Conf Proc*, 91–94
- Vandeweert E., Lievens P., Philipsen V., Bastiaansen J. and Silverans R.E. (2001): Measurements of the population partitions and state-selected flight-time distributions of keV ion-beam-sputtered metastable atoms. *Phys Rev B* **64**, 195417-12
- Wahl M. and Wucher A. (1994): VUV photoionization of sputtered neutral silver clusters. *Nucl Instrum Meth B* **94**, 36–46
- Wehner G.K. and Rosenberg D. (1960): Angular distribution of sputtered material. *J Appl Phys* **31**, 177–179
- Winograd N. (2005): The magic of cluster SIMS. *Anal Chem* **77**, 142A–149A
- Winograd N., Kobrin P.H., Schick G.A., Singh J., Baxter J.P. and Garrison B.J. (1986): Energy- and angle-resolved detection of neutral atoms desorbed from ion bombarded single crystals. Rh(111) and p(2*2)O/Rh(111). *Surf Sci* **176**, L817–L824
- Wittmaack K. (2003): Analytical description of the sputtering yields of silicon bombarded with normally incident ions. *Phys Rev B* **68**, 235211-1–11
- Wittmaack K. (2006): A critical review of the electron-tunneling model of secondary ion formation. *Mat Fys Medd Dan Vid Selsk* **52**,
- Wucher A. (1994): Internal energy of sputtered metal clusters. *Phys Rev B* **49**, 2012–2020
- Wucher A. (2002): Formation of clusters in Sputtering. *IZV An SSSR Fiz* **66**, 499–508
- Wucher A. (2006): Molecular secondary ion formation under cluster bombardment: A fundamental review. *Appl Surf Sci* **252**, 6482–6489
- Wucher A., Sun S., Szakal C. and Winograd N. (2004): Molecular Depth Profiling of Histamine in Ice using a Backmininster fullerence probe. *Anal Chem* **76**, 7234–7242
- Yu M.L. (1991): Charged and excited states of sputtered atoms. In: Behrisch R. et al. (Eds), *Sputtering by Particle Bombardment*, Vol. 3. Springer, Berlin, pp 91–160
- Yu M.L., Grischkowsky D. and Balant A.C. (1982): Velocity distributions of sputtered excited atoms. *Phys Rev Lett* **48**, 427–430